

**Acknowledgments:** We wish to thank the Defence Evaluation and Research Agency Malvern for the loan of a suitable GPS receiver. We also wish to thank the Jet Propulsion Laboratory of the California Institute of Technology for allowing us to use GPS Inferred Positioning SYstem Orbit Analysis and SImulation Software (GIPSY-OASIS II). We wish to thank United Kingdom Meteorological Office for access to radiosonde and synoptic measurements (supplied through the British Atmospheric Data Centre).

© IEE 1998

28 October 1998

Electronics Letters Online No: 19981661

O.T. Davies, R.G. Howell and P.A. Watson (Department of Electronic and Electrical Engineering, University of Bath, Bath BA2 7AY, United Kingdom)

E-mail: o.t.davies@bath.ac.uk

## References

- 1 FELDHAKE, G.: 'Estimating the attenuation due to combined atmospheric effects on modern earth-space paths', *IEEE Antennas Propagat. Mag.*, 1997, **39**, (4), pp. 26-34
- 2 DAVIES, O.T., and WATSON, P.A.: 'Comparisons of 93GHz radiometer predicted attenuation with integrated precipitable water vapour measured using GPS', *Electron. Lett.*, 1997, **33**, (25), pp. 2114-2116
- 3 SALONEN, E., and UPPALA, S.: 'New prediction method of cloud attenuation', *Electron. Lett.*, 1991, **27**, pp. 1106-1108
- 4 SALONEN, E., KARHU, S., JOKELA, P., ZHANG, W., UPPALA, S., AULAMO, H., and SARKKULA, S.: 'Study of propagation phenomena for low availabilities'. Final Report for ESA/ESTEC Contract 8025/88/NL/PR, 1990
- 5 LIEBE, H.J., HUFFORD, G.A., and COTTON, M.G.: 'Propagation modelling of moist air and suspended water/ice particles at frequencies below 1000GHz'. AGARD 52nd Specialists Meeting of the Electromagnetic Wave Propagation Panel, Palma De Mallorca, Spain, 1993, pp. 3/1-3/10
- 6 DAVIES, O.T., and WATSON, P.A.: 'Comparison of integrated precipitable water vapour obtained by GPS and radiosondes', *Electron. Lett.*, 1998, **34**, (7), pp. 645-646
- 7 Recommendation ITU-R P.676-3 'Attenuation by atmospheric gases'. ITU, 1997

## AuBe Ohmic contacts to *p*-type ZnTe

W.H. Lan, W.J. Lin, Yi-Cheng Cheng, K. Tai, C.M. Tasi, P.H. Wu, K.H. Cheng, S.T. Chou, C.M. Yang, Yi-Chang Cheng and K.F. Huang

Ohmic contacts of AuBe to *p*-ZnTe show a minimum specific contact resistance of  $3.0 \times 10^{-6} \Omega \text{cm}^2$  for a *p*-doping level of  $1.6 \times 10^{19} \text{cm}^{-3}$  and at an annealing temperature of  $200^\circ\text{C}$ . The beryllium is very effective at improving the electrical properties of *p*-type contacts to ZnTe.

II-VI wide bandgap semiconductors are being widely studied for optoelectronic devices [1]. ZnTe is a promising material because it can be doped with nitrogen in the region of  $10^{19} \text{cm}^{-3}$ . Much effort has been devoted to minimising the contact resistance [2-4]. To date, a minimum specific contact resistance of  $1.1 \times 10^{-6} \Omega \text{cm}^2$  has been obtained for ZnTe with an effective hole concentration  $3 \times 10^{19} \text{cm}^{-3}$  with Au/Pt/Ti/Ni metals by using an electron-beam coater [3]. In this Letter, we propose that gold-beryllium alloy (AuBe, 99:1, atm %), which can be evaporated easily in the thermal coater, is a good Ohmic metal for *p*-type ZnTe. The introduction of Be atoms led to a dramatic improvement in the Ohmic properties of *p*-type ZnTe.

ZnTe film was grown on a (001) semi-insulating GaAs substrate by MBE at  $280^\circ\text{C}$ . The source material was Zn(6N) and Te(6N). The *p*-type doping was carried out using a nitrogen plasma source. The hole concentration and mobility measured by the van der Pauw method were  $2.0 \times 10^{19} \text{cm}^{-3}$  and  $27 \text{cm}^2/\text{V}\cdot\text{s}$ . The thickness was  $0.66 \mu\text{m}$ . The specific contact resistance was measured by transmission line model (TLM) measurement. Before the formation of the TLM pattern, the sample was cleaned with methanol and de-ionised water. The TLM pattern was formed by a photoresist process. ZnTe mesa etching was carried out with  $\text{K}_2\text{Cr}_2\text{O}_7$ :

$\text{H}_2\text{SO}_4 : \text{H}_2\text{O}$  solution with an over-etch into the semi-insulating GaAs substrate. Using a normal lift-off process, the AuBe metal was deposited using a thermal coater after the surface oxide was removed by  $\text{HF} : \text{H}_2\text{O} = 1 : 200$  (volume ratio).

The length of the TLM pattern was 5, 8, 11, 13, 16, 19, 22,  $27 \mu\text{m}$  with a width of  $100 \mu\text{m}$ . Annealing was performed at various temperatures for 10min in a nitrogen gas ambient in a conventional furnace. The specific contact resistance was measured by using an hp3457A multimeter. The four-probe technique was used to avoid probe resistance effects.

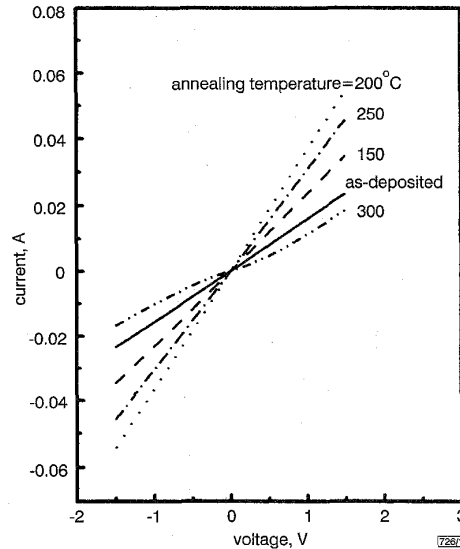


Fig. 1 Current-voltage (*I*-*V*) characteristic of top contact pad on pattern of transmission line model (TLM) measurement with linewidth  $100 \mu\text{m}$  and length  $27 \mu\text{m}$

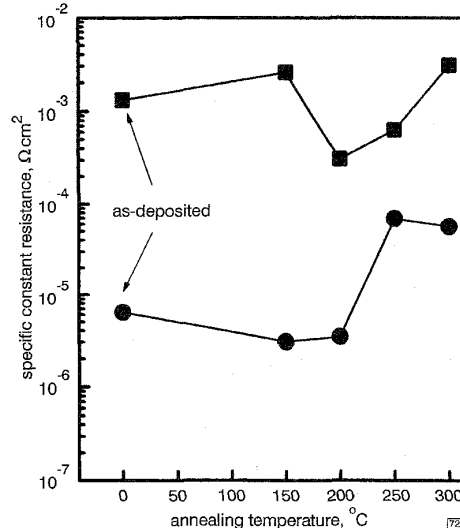


Fig. 2 Specific contact resistance of sample at different annealing temperatures

■ Au  
● AuBe

Fig. 1 shows the current-voltage (*I*-*V*) characteristic of the top contact pad on the pattern of the transmission line measurement with  $27 \mu\text{m}$  linewidth. The variations in the *I*-*V* characteristics caused by the annealing can be clearly observed in this Figure. Good Ohmic behaviour can be clearly observed in the as-deposited film as shown in Fig. 1. The specific contact resistance decreases as we increase the annealing temperature. Yet, as shown in Fig. 2, only a small decrease in the specific contact resistance ( $6.4 \times 10^{-6} - 3.0 \times 10^{-6} \Omega \text{cm}^2$ ) occurs while the annealing temperature is increased from the as deposited case to  $250^\circ\text{C}$ . While the

annealing temperature is  $> 300^\circ\text{C}$ , the specific contact resistance increases dramatically and some kinks in the I-V characteristic around 0.3V can also be observed. Thus, inferior Ohmic properties occurred under these annealing conditions. Since the Te out-diffusion behaviour can be observed in the XPS analysis, the degradation in Ohmic properties may be caused by the lack of Te in the ZnTe film. Further investigation is necessary to identify these characteristics.

We also compared the annealing effect of Au and AuBe. As shown in Fig. 2, the specific contact resistance of Au on *p*-type ZnTe varies in the range  $3.5 \times 10^{-3} - 3.0 \times 10^{-2} \Omega\text{cm}^2$  with different annealing temperatures. This result explains why different specific contact resistances were achieved in previous work [2, 3] with a similar layer structure. After the introduction of Be, an improvement in specific contact resistance of more than two decades was observed. The AuBe alloy is very effective at improving the electrical properties of *p*-type contacts to ZnTe.

In conclusion, Ohmic contacts formed from AuBe alloy provide a very low resistance to *p*-ZnTe. Specific contact resistances as low as  $3 \times 10^{-6} \Omega\text{cm}^2$  have been obtained after a  $200^\circ\text{C}$  annealing process.

© IEE 1998

13 October 1998

*Electronics Letters Online No: 19981563*

W.H. Lan and W.J. Lin (*Material R&D Center, Chung Shan Institute of Science and Technology, Taoyuan, Taiwan 325, Republic of China*)

Yi-Cheng Cheng and K. Tai (*Institute of Electro-Optical Engineering, National Chiao-Tung University, HsinChu, Taiwan 300, Republic of China*)

C.M. Tasi, P.H. Wu and K.H. Cheng (*Institute of Electro-Optical Science, National Taiwan Ocean University, Keelung, Taiwan 202, Republic of China*)

S.T. Chou, C.M. Yang and Yi-Chang Cheng (*Department of Electrical Engineering, Chung Cheng Institute of Technology, Taisi, Taoyan, Taiwan 335, Republic of China*)

K.F. Huang (*ElectroPhysics Department, National Chiao-Tung University, HsinChu, Taiwan 300, Republic of China*)

## References

- 1 HAASE, M.A., QIU, J., DEPUYDT, J.M., and CHENG, H.: 'Blue-green laser diodes', *Appl. Phys. Lett.*, 1991, **59**, pp. 1272-1274
- 2 TREXLER, J.T., FIJOL, J.J., CALHOUN, L.C., PARK, R.M., and HOLLOWAY, P.H.: 'Formation of ohmic contacts to *p*-ZnTe', *J. Electron. Mater.*, 1996, **25**, pp. 1474-1477
- 3 OZAWA, M., HIEI, F., TAKASU, M., ISHIBASHI, A., and AKIMOTO, K.: 'Low resistance ohmic contacts for *p*-type ZnTe', *Appl. Phys. Lett.*, 1994, **64**, pp. 1120-1122
- 4 MOCHIZUKI, K., TERANO, A., MOMOSE, M., TAIKE, A., KAWATA, M., GOTOH, J., and NAKATSUKA, S.: 'Au/Pt/Ti/Ni ohmic contacts to *p*-ZnTe', *Electron. Lett.*, 1995, **30**, pp. 1984-1985

## Bright electroluminescence from CdS quantum dot LED structures

S. Nakamura, K. Kitamura, H. Umeya, A. Jia, M. Kobayashi, A. Yoshikawa, M. Shimotomai, Y. Kato and K. Takahashi

Self-assembled quantum dots of CdS were introduced into the *pn* junction of ZnSe. Bright luminescence was observed at 77K and room temperature. The peak wavelength can be tuned by altering the dimensions of the quantum dot structure.

Heteroepitaxial growth of highly strained material systems has gained increasing interest as it offers the possibility of producing nanoscale structures such as self-assembled quantum dots (QDs) *in-situ* without any substrate patterning process [1, 2]. Although QD size fluctuations, inherent in the growth process, result in inhomogeneous electrical and optical properties, the self-assembly of strain-induced islands provides the means for creating zero-dimensional quantum structures without having to overcome the current limitations of lithography. In addition, they offer the opportunity to study and test novel device physics [3]. Because II-

VI materials typically have wider bandgaps and stronger exciton-photon interactions than III-V materials, II-VI semiconductor nanostructures are expected to be very useful in exploring the exciton nature in low-dimensional structures. Self-assembled quantum dots of CdS were examined in this study as a novel QD system grown by MBE. It was found recently that CdS QD shapes can be made either circular or rectangular depending on the growth conditions [4]. The controllability of the shape is probably related to a metastable crystallographic feature of CdS; hexagonal structure or cubic structure epilayers could be selectively grown on (001) GaAs substrates through small changes in the growth conditions [5]. In this study, the optical properties of the QD samples were mainly characterised by low temperature (13K) photoluminescence (PL). CdS QD layers were also embedded in the *pn* junction of ZnSe and the device performance was characterised.

CdS dots on (001) ZnSe surfaces were fabricated in an MBE machine equipped with elemental sources. An elemental sulphur beam was supplied by a valve cracker cell. A ZnSe buffer was grown at  $300^\circ\text{C}$  on (001) GaAs substrate with a thickness of  $1000\text{\AA}$  or less; the ZnSe buffer layer thickness was maintained within the critical layer thickness so that misfit dislocations did not affect the nucleation of QDs. The dots were grown by simultaneously opening both Cd and S shutters. The nominal growth rate of CdS was deduced using the growth rate of CdS thin films and it was reduced to  $\sim 0.03\text{ML/s}$ . PL was measured from the CdS QD samples without the need for capping layers. This is a unique feature of the CdS QD system on ZnSe; other QD systems usually require the formation of cap layers before PL measurements can be carried out. The existence of the cap layer for the CdS QD system does not affect its PL spectrum, but the PL peak intensity could be improved by an order of magnitude. A single peak and strong luminescence with relatively wide linewidth were observed.

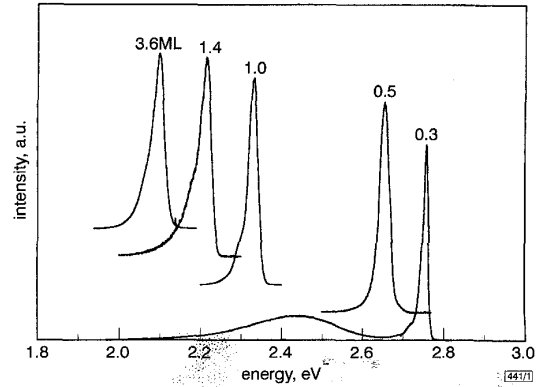


Fig. 1 PL spectra of various QD samples obtained at 13K

Fig. 1 shows variations in the PL spectra with respect to variation in the CdS deposition. When the deposited CdS corresponded to 0.5ML, the PL peak at 13K was located at 2.65eV and the FWHM was 29m eV. Since neither the ZnSe epilayers nor CdS epilayers showed such a spectrum, the PL can be associated with the CdS nanostructures. As was observed in other QD systems, a blue shift was obtained by depositing a thinner layer of CdS. A QD sample in which the CdS deposition was 3.6 ML has a peak at  $\sim 2.10\text{eV}$ , and the sample in which the CdS deposition corresponds to 1.4ML has a peak at  $\sim 2.21\text{eV}$ . Further reductions in the deposition of CdS shifted the luminescence colour towards the blue end of the spectrum. Green luminescence, with a peak of  $\sim 2.33\text{eV}$ , was observed when the CdS deposition was  $\sim 1.0\text{ML}$ . Bright blue luminescence, with a peak of  $\sim 2.76\text{eV}$ , was observed when the CdS deposition was  $\sim 0.3\text{ML}$ . The PL peak position varied from sample to sample, and covered a higher energy range of the CdS bandgap to a lower energy range. This is probably related to the band line-up between ZnSe and CdS. The band line-up between bulk ZnSe and bulk CdS is considered to be of type II, and this characteristic nature would contribute to the wide tunable range of the PL peak energy. Studies to obtain detailed characteristics including a time resolved study are currently being carried out.

The CdS QD was included in the ZnSe *pn* junction device. As shown in Fig. 2, a (001) oriented *n*-GaAs substrate was used and 1  $\mu\text{m}$  thick *n*-ZnSe layers ( $n = 5 \times 10^{17} \text{cm}^{-3}$ ) was grown directly on